Eidgenössische Technische Hochschule Zürich
Swiss Federal Institute of Technology Zurich

Lecture with Computer Exercises: Modelling and Simulating Social Systems with MATLAB

Project Report

Turing Patterns from Dynamics of Early HIV infection

Jorge Bretones Santamarina

Zürich
December 2017

ETH

Eidgenössische Technische Hochschule Zürich
Swiss Federal Institute of Technology Zurich

Declaration of originality

The signed declaration of originality is a component of every semester paper, Bachelor's thesis, Master's thesis and any other degree paper undertaken during the course of studies, including the respective electronic versions.

Lecturers may also require a declaration of originality for other written papers compiled for their courses.

I hereby confirm that I am the sole author of the written work here enclosed and that I have compiled it in my own words. Parts excepted are corrections of form and content by the supervisor.

Title of work (in block letters):

TURING PATTERNS FROM DYNAMICS OF EARLY HIV INFECTION

Authored by (in block letters):

For papers written by groups the names of all authors are required.

Name(s):	**First name(s):**
BRETONES SANTAMARINA	JORGE

With my signature I confirm that

- I have committed none of the forms of plagiarism described in the 'Citation etiquette' information sheet.
- I have documented all methods, data and processes truthfully.
- I have not manipulated any data.
- I have mentioned all persons who were significant facilitators of the work.

I am aware that the work may be screened electronically for plagiarism.

Place, date	**Signature(s)**
ZURICH, 16/12/17	Jorge B.

For papers written by groups the names of all authors are required. Their signatures collectively guarantee the entire content of the written paper.

Agreement for free-download

We hereby agree to make our source code of this project freely available for download from the web pages of the SOMS chair. Furthermore, we assure that all source code is written by ourselves and is not violating any copyright restrictions.

Jorge Bretones Santamarina

Table of contents

1. Abstract

The application of Turing Patterns to the field of biology has long been investigated since the famous British mathematician formulated his theory, well-known for its multiple scientific applications and especially for its contributions to the field of embryonic development. Nevertheless, Turing's mathematical insights about reaction-diffusion systems have been proved to apply to numerous biological problems. In the current report we will address an immunological question, namely if an extension of a classical SIR model including both diffusion and chemotaxis can lead to the appearance of hot spots of infection during early HIV infection in the vaginal epithelium. The analysis has been conducted regarding the mucosa as a 1D domain in which lymphocytes T, infected cells and virions might react and diffuse. Throughout the simulation and posterior analysis, irregularities in the author's results have been encountered and complications have been experienced while trying to replicate the findings. Accordingly, this raises concerns about the quality of computational publications and about the difficulties of reproducing published scientific papers.

2. Individual contributions

Jorge Bretones Santamarina conducted the bibliographic research, implemented the model, analysed the results and wrote the report.

3. Introduction and Motivations

3.1 HIV infection and immunological response

The human immunodeficiency virus (HIV) is an RNA virus that belongs to the *lentivirus* genus of the *retroviridae* family. The members of this family are well-known for encoding a reverse transcriptase, an enzyme capable of synthesizing DNA from an RNA template. Moreover, with the aid of an integrase, they can insert the newly produced DNA into the host's genome [1]. There are two main HIV types in humans: type 1 and 2 and recent evidence shows that both of them arose from zoonotic events of more than 20 strains of SIV (Simian Immunodeficiency Virus) [2].

Viruses of the genus *lentivirus* infect mammals and HIV infects specifically humans, being transmitted by corporal secretions (blood, semen…etc.). Upon infection, the virus targets the CD4 glycoprotein receptor of the membrane of the lymphocytes T of the CD4+ series. Those are the immune cells in charge of the adaptive immune response, whose activation is necessary to coordinate the actors of the innate response, as well as for the generation and maturation of antibody-producing plasma B cells [3]. Once inside the cell and being integrated into the host DNA, HIV might remain silent for long periods of time, but once activated it uses the cellular machinery to produce more copies of itself, thus inducing the lysis of the T-CD4 lymphocytes [4]. Therefore, an HIV infection is detected usually due to a wide systemic immunosuppression, which if not treated with HAART (Highly Active Antiretroviral Therapy)[1] will lead to a dramatic decrease in the T-cell blood count of the patient and eventually to the death of the host [5].

Since the epidemic outbreak in the 80s, HIV has posed an important challenge to the healthcare and scientific community. The lack of use of disposable syringes among drug users and of means to prevent the spread of sexually transmitted infections (STIs) explains the expansion of the disease in countries like Switzerland. Recent phylogenetic studies have proved that prevention strategies for drug users have provoked a substantial drop in the HIV-1 infected cluster in Switzerland, thus proving the efficiency of control methods [5].

HIV type 1, the most common cause of AIDS in humans, is responsible for the infection of more than 50 million people, with an average number of 6 million infections per year [6]. By the end of 2016, according to the World Health Organisation (WHO), 36.7 million people lived with HIV and 20.9 million people were receiving antiretroviral therapy [7].

Given the importance of this viral disease, the publication that motivated this report [8] is understood as one of the multiple pieces of research that have tried to gain a deeper insight into the viral infection process, given the importance that eradicating this virus could have at a global scale.

[1] HAART includes a combination of drugs that simultaneously target different molecular mechanisms of the HIV virus, for instance, the RT, the integrase, the protease or membrane glycoproteins necessary for the de-encapsulation and entry of the virus into the cell [5].

3.2 Turing instability and reaction-diffusion systems

The theoretical description of patterning developed by Allan Turing in his publication "Chemical basis of morphogenesis" (1952) [9] revolutionized the way of understanding embryology, defined as "the part of biology which is concerned with the formation and development of the embryo from fertilization until birth". More specifically, morphogenesis is interested in the development of patterns and forms, which are promoted by the diffusion and reaction of molecules in spatial domains along time [10].

An interesting theory for pattern formation is called "positional information", in which L. Wolpert proposed that cells can react to morphogen concentrations and differentiate into diverse lineages. Thus, albeit the pattern formation process remains unknown at present time, upon formation of morphogen spatial patterns, cells are able to read out their position according to the local concentration and trigger a particular genetic expression program which will determine a certain cellular fate [11].

In the mid-fifties, Turing set the basis for the reaction-diffusion equation, stating that steady state heterogeneous spatial patterns of morphogen concentration could be generated upon reaction and diffusion of chemical species:

$$\frac{\partial A}{\partial t} = F(A, B) + D_A \cdot \nabla^2 A$$

$$\frac{\partial B}{\partial t} = G(A, B) + D_B \cdot \nabla^2 B$$

Where F and G are non-linear kinetics.

Turing proposed that if diffusion is not present (D_A, D_B = 0), then A and B will form a linearly stable uniform steady state. Nonetheless, upon inclusion of diffusion and if D_A differs enough from D_B, spatially inhomogeneous patterns can evolve due to the existence of diffusion driven instability [10].

3.3 Turing patterns and HIV infection dynamics

The paper which we are basing this project on, approaches an immunological problem from a new spatio-temporal perspective based on the inclusion of the reaction diffusion equation into a typical SIR immunological disease model. According to the authors, most of the previous HIV mathematical models did not account for spatial behaviour in the early spread of the virus, thus assuming a well-mixed non-realistic environment [8]. They claim that one possible source of spatial heterogeneities can be the infectious dynamics, which can be assumed to behave as a Turing system. Furthermore, they consider the presence of chemotaxis in the model, as a way to account for the chemical attraction of T cells to the site of infection by a gradient of cytokines [8].

As explained in section (3.2), with such a setting, a spatially homogeneous steady state in the absence of diffusion and chemotaxis would become linearly unstable when the system is coupled to both processes. For some choice of parameters, the SIR-Turing model can be shown to exhibit hot spots of infection in the vaginal epithelium [8].

Therefore, the goal of this project is to reproduce the results of the publication and to check whether with the information provided, it is possible to obtain Turing Patterns in a dynamical system with three species that react and diffuse in a 1D spatial domain. In this regard, the software MATLAB 2017b and its built-in PDE solver *pdepe* will be used to numerically solve the system of equations and analyse the results.

4. Description of the Model

The model considered in the paper is a standard SIR model (S = Susceptible; I = Infected; R = Recovered) for in-host virus dynamics in which we have three dependent variables:

T → uninfected T-CD4+ cells.

I → infected cells.

V → free virions.

The initial temporal dynamics are modelled by an ODE approach:

$$\frac{dT}{dt} = s - kVT - \mu T$$

$$\frac{dI}{dt} = kVT - \delta I$$

$$\frac{dV}{dt} = NI - cV$$

However, in such a system, spatial changing dynamics are not regarded, so diffusion and chemotaxis terms were included, thus yielding a system of PDEs which accounts for spatio-temporal effects in the disease dynamics:

$$\frac{\partial T}{\partial t} = s - kVT - \mu T + D_T \cdot \nabla^2 T - \chi \nabla(\mathrm{T}\nabla \mathrm{I})$$

$$\frac{\partial I}{\partial t} = kVT - \delta I + D_I \cdot \nabla^2 I$$

$$\frac{\partial V}{\partial t} = NI - cV + D_V \cdot \nabla^2 V$$

Where now T, I and V represent concentrations of the respective cellular types with the corresponding units measured in cells · mm, as we will be simulating in a 1D domain.
In addition, the parameter values were extracted from previous studies that included experimental measures of HIV in-host dynamics:

Parameter symbol	**Value and units**	**Biological meaning**
s	10 cells · mm^{-3} · day^{-1}	Target cells (T) supply rate
k	$3.43 \cdot 10^{-5}$ ml · $virion^{-1}$ · day^{-1}	Rate of infection of T cells
μ	0.03 · day^{-1}	T cells death rate
δ	0.5 · day^{-1}	Infected cells (I) death rate
N	480 virions · $cell^{-1}$ · day^{-1}	Virions production rate in I cells
c	3 day^{-1}	Clearance rate of virions
D_T	0.09504 mm^2 · day^{-1}	Diffusion coefficient of T cells
D_I	0.09504 mm^2 · day^{-1}	Diffusion coefficient of I cells
D_V	0.00076 mm^2 · day^{-1}	Diffusion coefficient of virions
L	1.78 mm	Length of the spatial domain

Finally, a non-dimensionalization was applied to the system in order to simplify it and facilitate the computation:

$$\xi = \frac{skN}{c\delta\mu};\ d_I = \frac{D_I}{D_T};\ d_V = \frac{D_V}{D_T};\ d_\chi = \frac{s\chi}{\delta D_T}\left(1 - \frac{1}{\xi}\right);\ \alpha = \frac{\delta}{\mu};\ \beta = \frac{c}{\mu}$$

Applying the non-dimensional parameters to our system, we get the final system of equations:

$$\frac{\partial u_1}{\partial \tau} = \xi - (1-\xi)\,u_1 u_3 - u_1 + \nabla^2 u_1 - d_\chi \nabla(u_1 \nabla u_2)$$

$$\frac{\partial u_2}{\partial \tau} = \alpha(u_1 u_3 - u_2) + d_I \nabla^2 u_2$$

$$\frac{\partial u_3}{\partial \tau} = \beta(u_2 - u_3) + d_V \nabla^2 u_3$$

Where now u_1 equals the non-dimensional concentration of T cells, u_2 of infected cells and u_3 of free virions. The letter τ represents the non-dimensional time.

In order to explore the steady states of the given system, a situation in which there is no spatial variation must be considered (every time derivative equals 0). There are thus two possibilities:

1. Endemic spatially homogeneous steady-state: (u_1^*, u_2^*, u_3^*) = (1, 1, 1). This case fulfils the condition of zero derivatives and it shows a positive concentration of T cells, infected cells and virions, thus the system stabilizes around a disease steady state (as infected cells and virions are represented).

2. Disease-free spatially homogeneous steady state: (u_1^*, u_2^*, u_3^*) = (ξ, 0, 0). The condition to achieve a fixed point is also fulfilled but in this case the steady state only includes a concentration of uninfected T cells. In this state we can distinguish 2 situations:

-If $\xi < 1$ we get negative values for I and V, so the solution is not physically relevant.

- If $\xi > 1$, the disease-free steady state is relevant.

Now, in order to check if Turing patterns can emerge in the surroundings of either of the two considered steady states, a linearization of the final system of equations around both of them is performed. A small perturbation around the steady state is considered and the eigenvalues of the matrix of coefficients (Jacobian matrix) are analysed to determine if

the real parts are positive (which would indicate divergent evolution from the steady state and thus Turing instability):

A. The linear stability analysis around the endemic state (1, 1, 1) shows that:

In the absence of diffusion and chemotaxis (only temporal variation), the steady state is stable, so the first condition for a Turing Pattern is fulfilled. In presence of spatial variation a series of three parametric conditions for Turing instability are derived (see [8]). We will just focus on the fulfilment of the weakest of the three. That is condition (C2), which has the following form:

$$d_\chi \geq \frac{\xi \cdot d_v}{\beta} + \frac{\xi \cdot d_I}{\alpha}$$

This formula will be especially relevant for the results, as it specifies the lower bound for the chemotactic threshold (χ) needed to achieve Turing patterns in our system.

B. Linearization around the disease free steady state (ξ, 0, 0) indicates that:

In the absence of spatial variation, only a negative ξ makes the steady state stable, thus meeting the first Turing condition. Nonetheless, even in the presence of chemotaxis and diffusion, the trace of the matrix of coefficients is negative, while the determinant is positive, so we fulfil the condition to obtain a stable node. Accordingly, Turing instability cannot arise and in the neighbourhood of the disease free steady state and Turing patterns cannot be obtained.

Finally, after determining the possible steady states for our dynamical system, linearizing our system around them and exploring the fulfilment of both Turing conditions, we will implement the model in order to test the results.

5. Implementation

5.1 Introduction to the Finite-Difference Method (FDM)

The model was implemented in the software MATLAB 2017b using the PDE toolbox including the function *pdepe* to solve systems of Partial Differential Equations (PDEs). As for numerous PDE systems, analytical solutions are hard to obtain or even impossible, so numerical solutions must be considered. The build-in solver employs the Finite-

Difference Method (FDM), whose goal is to find an approximation to a function that gives a relationship between its derivatives on some spatio-temporal region and under some boundary conditions. In Finite-Difference, the derivatives are replaced by finite difference approximations based on values of the function at discrete points [12].

As an illustrative example, we will consider a smooth function u (x) that we would like to approximate. To approximate $u'(x_1)$, the value of the derivative at a near point x_1, we would use:

$$D_+u(x_1) = \frac{u(x_1 + h) - u(x_1)}{h}$$

Or

$$D_-u(x_1) = \frac{u(x_1) - u(x_1 - h)}{h}$$

Or

$$D_0u(x_1) = \frac{u(x_1 + h) - u(x_1 - h)}{2h} = \frac{1}{2}(D_+u(x_1) + D_-u(x_1))$$

Where h is a small value. D_+ u (x_1) is the slope of the line interpolating u at points x_1 and x_1 + h (to the right of point x_1) and D_- u (x_1) is the same but for points located left of our reference point. D_0 u (x_1) is the so called "centered approximation", with a lower error than the other two approximations. Figure 1 depicts the Finite Difference Approximation:

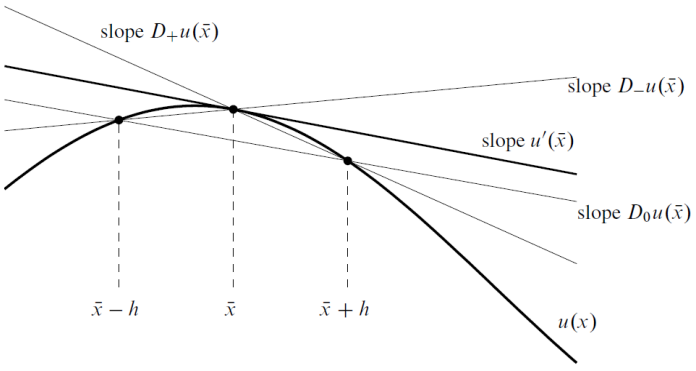

Figure 1: Finite-Difference Approximation, taken from [12]. Three approximations to the derivative of u at a point x are shown, being interepreted as the slope of secant lines.

5.2 Finite-Difference Method in MATLAB: PDE Toolbox

The PDE toolbox included in MATLAB can solve numerically systems of PDEs (either parabolic or elliptic) in 1 spatial dimension (x) and through time (t) [13]. In order to obtain the solution, we ought to create 4 different functions, each of them giving a piece of information to the solver. In this project we named our functions "TuringImmuno" (for more information, see the code attached). There are four of them:

1. TuringImmuno.m: it is the main function, in which we define our parameter values, write a call to the pdepe solver and include the plots and analytical tools which will be used after computing the solution.

2. TuringImmunoPDEfun.m: in this file we just need to encode our system of PDEs in a way that MATLAB can understand, namely:

$$c\left(x,t,u,\frac{\partial u}{\partial t}\right)\frac{\partial u}{\partial t}=x^{-m}\frac{\partial}{\partial x}\left(x^{m}f\left(x,t,u,\frac{\partial u}{\partial x}\right)\right)+s\left(x,t,u,\frac{\partial u}{\partial x}\right)$$

Coefficient "m" determines the geometry of the problem, which is "slab" in this time, so we have m set to 0. The following observations must be considered:

-Term "c" will equal to 1 in all our equations, as we have no term multiplying the derivative.

-Term "f" will contain the diffusion terms, as it implicates the second derivative of our concentrations with respect to space, as well as the chemotaxis term for species u_1, as it contains a multiplication of a first and a second derivative.

-Term "s" will contain the rest of the terms in the equations: parameters like α and β multiplying the variables (no first or second spatial derivatives).

3. TuringImmunoICfun.m: in this simple function we create a vector in which we input the initial concentrations of our 3 species. More specifically, values around the point (1, 1, 1) have been considered, as they represent small perturbations around the endemic steady state. As explained in part (4), this is the only steady state relevant for the formation of Turing patterns due to the existence of diffusion and chemotaxis driven instability.

4. TuringImmunoBCfun.m: this function defines the boundary conditions on x = a (being usually a = 0) and x = L (L = length of the spatial domain), which basically

determine if, for each of the species considered, there is a flux at the boundaries (E.g.: du/dt has a non 0 value) or there is a certain concentration (E.g.: u (0, t) = c0 or u (L, t) = c0). As for the PDEs, the boundary conditions must also be encoded in a particular manner:

$$p(x,t,u) + q(x,t)\, f\left(x,t,u,\frac{\partial u}{\partial x}\right) = 0$$

Thus, we have terms: pl, ql, pr and qr, that define the application of functions p and q to xl (leftmost point of the domain) and xr (rightmost point), respectively. In the paper, zero flux BCs are specified at both ends of the 1D domain and no fixed concentrations are imposed. Thus:

-Function "p" needs to be 0 to satisfy our conditions. Therefore, pl, pr = 0.

-Thus, "q" is going to be set to 1, so that when it multiplies f (f = du/dx = 0), we get 0 at the right hand side. Thus, ql, qr = 1.

(For more information regarding this issue, check the MATLAB code provided).

6. Simulation Results and Discussion

Firstly, in order to simulate from different initial conditions and values of the effective chemotaxis term (χ), all parameters needed to be encoded into MATLAB. Regarding parameters s and k (see section (4)), both are volume dependent, as their units are expressed in mm^3 and ml, respectively. In order to achieve volume independence in 1D, the authors suggest that they must be both multiplied by h^2, being h = 0.1 mm the thickness of the spatial domain. In the case of parameter s, this leads to a correct result expressed in mm:

$$\tilde{s} = s \cdot h^2 = \frac{10\ cells}{mm^3 \cdot day} \cdot (0.1\ mm)^2 = \frac{0.1\ cells}{mm \cdot day}$$

Nevertheless, for parameter k it leads to a huge error in the units:

$$\tilde{k} = k \cdot h^2 = \frac{3.43 \cdot 10^{-5}\ ml}{virion \cdot day} \cdot \frac{1000\ mm^3}{1\ ml} \cdot (0.1\ mm)^2 = 3.43 \cdot 10^{-4}\ \frac{mm^5}{virion \cdot day}$$

The red colour has been used to indicate that the result is wrong, as we get mm^5 and not mm. Instead, if we divide k by h^2 we get the following:

$$\tilde{k} = \frac{k}{h^2} = \frac{3.43 \cdot 10^{-2} \ \frac{mm^3}{virion \cdot day}}{(0.1\,mm)^2} = 3.43 \ \frac{mm}{virion \cdot day}$$

In this case, it is easy to observe that both parameters are expressed in the right units and in the following section we will see that with this correction we are able to relate d_χ and χ correctly and the same way the authors do.

Secondly, in order to reproduce the results let's come back to our weakest condition for the achievement of Turing instability in our system (see section (4)):

$$d_\chi \geq \frac{\xi \cdot d_v}{\beta} + \frac{\xi \cdot d_I}{\alpha}$$

As the non-dimensional parameters α, β, ξ, d_v and d_I depend entirely in our choice of parameters, applying the corresponding values we obtain that d_χ needs to be equal or bigger than 219.8.

Thus, we just need to plug this value into the formula of d_χ and subtract the value of the lower bound of the chemotaxis threshold (χ). As we prove in our MATLAB script, the minimum value necessary to achieve Turing Patterns is $\chi > 104$ mm^3 $cell^{-1}$ day^{-1} (units for 1D), the same value the authors obtain.

Before moving onto the simulation results, there are a few aspects about the way results are presented in the paper that we would briefly like to comment:

1. Most of the Figures include a simulation at non-dimensional time $\tau = 0.00$. Given that the formula for τ is the following:

$$\tau = \frac{t}{Tc} = \frac{t}{33.33\ day}$$

The only possibility for τ to be 0.00 is if $t = 0.00$. Therefore, we were unable to reproduce all results under this particular condition, as the PDE solver in MATLAB needs a positive time to let the system evolve and perform the integration accordingly.

2. The initial conditions are not always stated clearly and must be thus inferred from the Figures, something not precisely accurate. Particularly, in the case of Figure 3 it is said that the same initial conditions as Figure 2 are employed. However, that is not what we observe judging from the plots. Given the importance of initial conditions to solve

correctly these type of systems, we are aware that this inconsistencies might lead to the wrong results in our simulations.

Concerning the actual results, as it is proved in the paper, for values of χ under 104 mm^3 $cell^{-1}$ day^{-1} solutions have a flat shape as time goes by. We were able to reproduce results from Figure 2* (see Figure 2).

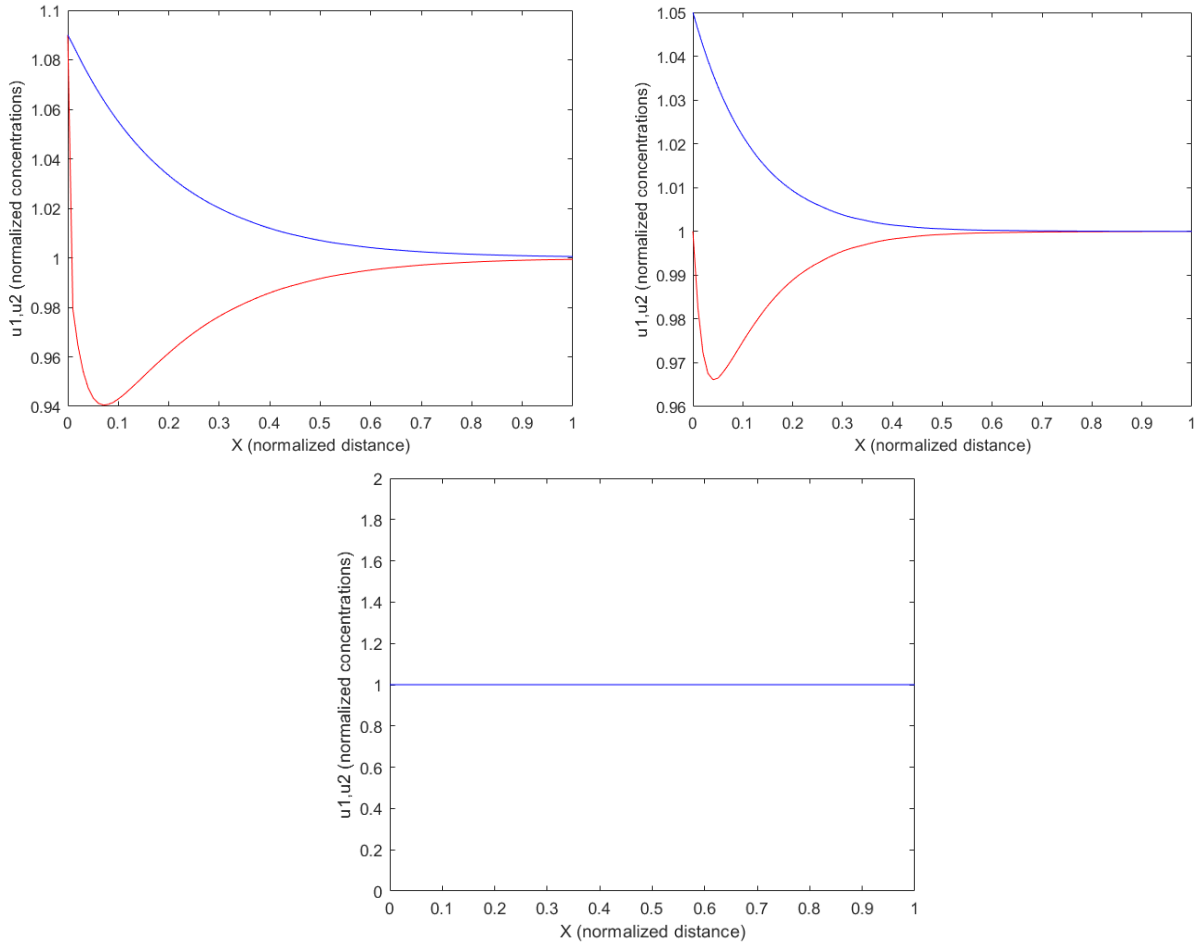

Figure 2: timeseries are represented by a red line (for u_1) and a blue one (for u_2). The concentration of u_3 is initially equal to 1 in all cases, as presented in the paper. **B.** Corresponds to Fig.2B of the paper. The initial conditions were taken as both u_1 (0, x) = u_2 (0, x) = 1.09 and simulation time τ = 0.3. **C**. Corresponds to Fig. 2C of the paper. In this case u_1 (0, x) = 1, u_2 (0, x) = 1.05 and τ = 0.5. **D.** Corresponds to Fig. 2D of the paper. The initial conditions were taken as: u_1 (0, x) = u_2 (0, x) = u_3 (0, x) = 1 and τ = 2.

As we observe in the pictures, when initial conditions are picked as a small perturbation around the endemic steady state (1, 1, 1) with a value of $\chi < 104$ mm^3 $cell^{-1}$ day^{-1}, a flat solution is obtained and no Turing pattern arises (Figure 2). We could reproduce the

shape of these figures from the paper using 100 Δts and 100 Δxs (defect value for the linspace function in MATLAB).

Moving onto Figure 3, on page 784 of the paper it is claimed that Turing patterns are observed in the form of three separated peaks (no flat solution) using a value of $\chi = 130$ mm^3 $cell^{-1}$. This is striking, as on page 783 it is literally stated: "Turing conditions are only met for χ somewhere between 110 and 120 mm^3 $cell^{-1}$ day^{-1}". To see whether this affirmation is true or not, we simulated with 100 time steps and 100 grid splits and got a flat solution.

However, after a close examination of the model and a large number of simulations varying number of Δts and Δxs, we have been able to replicate the appearance of oscillations in Figures 3, 4 and 5. That is the proof that the model is intrinsically correct, but the absence of a clear input for the integration steps and initial conditions determines the presence of instability in the solutions.

In this regard, in Figure 3 we obtain oscillations and thus Turing patterns for a value of $\chi = 130$ mm^3 $cell^{-1}$ day^{-1}. In Figure 4 we increased χ up to 170 mm^3 $cell^{-1}$ day^{-1} (not to 220 just to save computational power) and we doubled the size of the domain, proving that the spikes become steeper for higher chemotaxis. In Figure 5 we increased the size of the x grid four times and got more spikes, all roughly the same high (steady state).

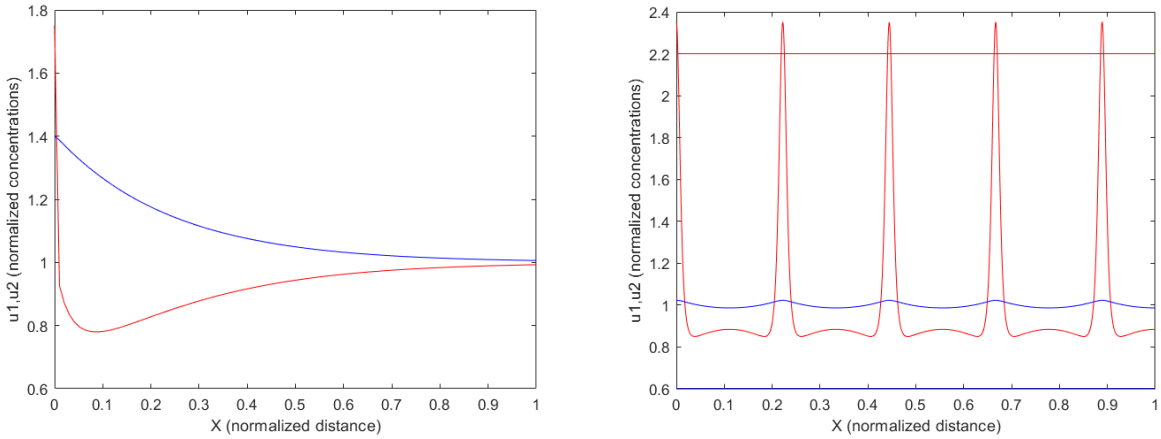

Figure 3: same colour code as Fig. 2. **B**. Corresponds to Fig. 3B of the paper. We used u_1 (0, x) = 1.75, u_2 (0, x) = 1.4 and $\tau = 0.25$. The number of Δt and Δx is 100 in both cases. **C**: Corresponds to a long time simulation in which we chose Δt = 11 and Δx = 1001. We employed u_1 (0, x) = 2.2, u_2 (0, x) = 0.6 and τ = 1000.

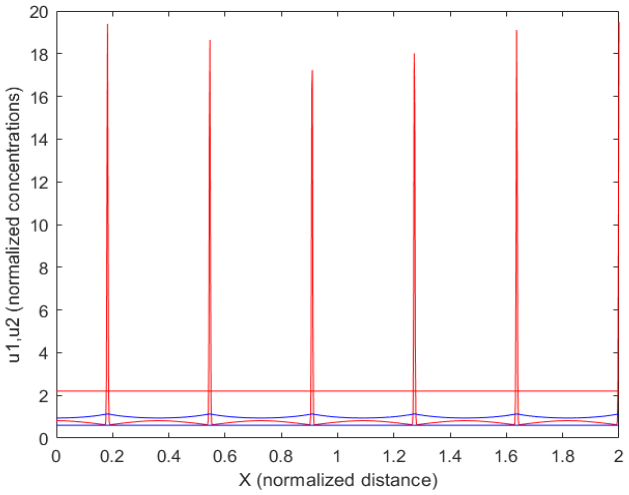

Figure 4: same code colour as Fig.2. Here we increased the strength of chemotaxis χ up to 170 mm^3 $cell^{-1}$ day^{-1} and doubled the size of the domain. We used u_1 (0, x) = 2.2, u_2 (0, x) = 0.6 and τ = 1000. Spikes get thinner compared to Fig. 3.

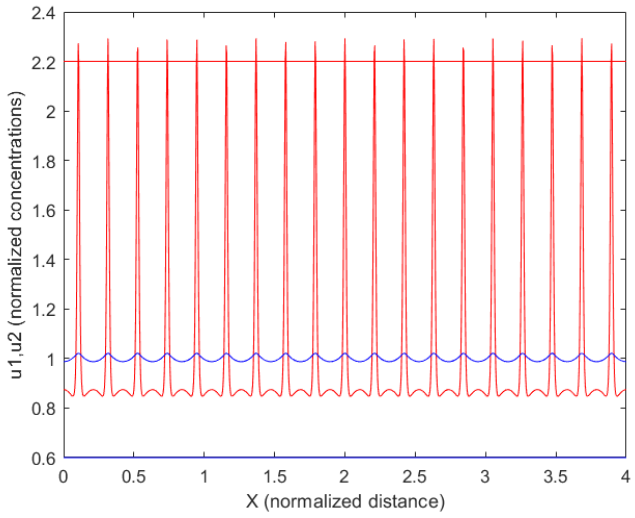

Figure 5: same code colour as Fig.2. We come back to χ = 130 mm^3 $cell^{-1}$ day^{-1} but the length of the domain has been increased by four. We used u_1 (0, x) = 2.2, u_2 (0, x) = 0.6 and τ = 1000. Very little variation is appreciated in the peaks high.

These results demonstrate that, in order to be able to replicate a simulation of this kind, knowing the relationship between the number of time steps and x steps is paramount. The multiple simulations conducted have shown that little variations of even 1 unit in one of both values determines that the solution shape changes abruptly. Thus, we can conclude

that without knowing the exact values employed by the authors it is nearly impossible to replicate their results.

Nonetheless, regardless of that, we have been able to demonstrate that hot spots of infection arise due to the existence of Turing instability in the presence of diffusion and chemotactic attraction higher than 104 mm^3 $cell^{-1}$ day^{-1}.

7. Summary and Outlook

The main topic covered in this report is the application of the reaction-diffusion equations to an immunological question, namely the behaviour of the HIV virus during the primary infection in a 1D domain representing the vaginal/anal epithelium. After examining the relevance and broad applicability of Turing's reaction-diffusion equation, we have added it to a classical SIR model along with a chemotaxis term, in order to account for spatio-temporal variation of the components and the effect of chemical attraction in T cells diffusion.

Then, we have addressed the conditions of Turing's instability in our system and concluded that only in the surrounding of the endemic steady state patterns may arise, always in presence of a certain level of chemotaxis and diffusion.

In order to corroborate the results of the paper a large number of simulations have been conducted. On the whole, the results obtained by the authors have been replicated, showing that for values of the chemotaxis threshold small enough, Turing instability does not arise and flat solutions appear. Conversely, for higher values and certain initial conditions, Turing patterns appear in the form of oscillations of all components (especially of u_1, who has the chemotaxis term attached).

Apart from this obvious remarks, the problems encountered during the execution of this project have brought up some important issues that must be commented:

1. The lack of information about the number of time steps and spatial domain partitions is of special importance for the PDE solver. Ignoring these values makes it extremely difficult to replicate results, thus raising concerns about the replicability of publications as the one motivating this project.

2. The misspecification of initial conditions is highly relevant as well. As observed throughout the simulations, a little change in the starting concentration of one of the

species can have dramatic consequences in the output. A table with a proper list of the initial concentrations employed in every simulation would be helpful.

3. Checking the parameter units might be helpful in order to detect potential mistakes during parameter non-dimensionalization.

4. Publishing the code with the paper is, from our perspective, a practice that would urgently need to become more widespread, as it helps eliminating barriers in scientific communication.

Finally, albeit the difficulties and problems stated above, the originality and innovative character of the model must be admitted. As far as we are concerned, this investigation applies a novel approach to a problem as studied as HIV. In this regard, coming up with new approaches considering spatio-temporal variations of components inside the host can help understand the evolution in time and space of the infectious process. This, complemented with molecular and epidemiological evidence, might be extremely useful to help unravel the whole mechanism of viral infection, thus paving the way for the potential development of therapies or preventive procedures.

8. References

1. Coffin JM, Hughes SH, Varmus HE, editors. Retroviruses. Cold Spring Harbor (NY): Cold Spring Harbor Laboratory Press; 1997.

2. Hahn BH, Shaw GM, De KM, Sharp PM. AIDS as a zoonosis: scientific and public health implications. Science. 2000 Jan 28;287(5453):607–14. pmid:10649986

3. Alberts B, Johnson A, Lewis J, et al. Molecular Biology of the Cell. 4th edition. New York: Garland Science; 2002. Chapter 24, The Adaptive Immune System.

4. Pegu A, Asokan M, Wu L, Wang K, Hataye J, Casazza JP, et al. Activation and lysis of human CD4 cells latently infected with HIV-1. *Nat Commun* (2015) 6:8447. doi:10.1038/ncomms9447.

5. Pau A. K., George J. M. (2014). Antiretroviral therapy: current drugs. Infect. Dis. Clin. North Am. 28, 371–402. 10.1016/j.idc.2014.06.001.

6. Kouyos RD, von Wyl V, Yerly S, Böni J, Taffé P, Shah C, et al. Molecular epidemiology reveals long-term changes in HIV type 1 subtype B transmission in Switzerland. J Infect Dis. 2010;201(10):1488–97. pmid:20384495.

7. World Health Organization (WHO). Internet resource consulted on the 12/12/2017 at http://www.who.int/hiv/en/

8. Stancevic, O.; Angstmann, C.N.; Murray, J.M.; Henry, B.I. Turing patterns from dynamics of early HIV infection. Bull. Math. Biol. 2013, 7, 774–795.

9. Turing, A. M. (1952). "The Chemical Basis of Morphogenesis". Philosophical Transactions of the Royal Society of London B. 237 (641): 37–72. doi:10.1098/rstb.1952.0012.

10. Murray JD (1993) Mathematical biology. Springer, New York.

11. Wolpert L. Positional information and the spatial pattern of cellular differentiation. J. Theor. Biol. 1969;25:1–47. doi: 10.1016/S0022-5193(69)80016-0.

12. R. J. LeVeque, Finite Difference Methods for Ordinary and Partial Differential Equations, Society for Industrial and Applied Mathematics (SIAM), 2007.

13. PDF Documentation for Partial Differential Equation Toolbox. Online resource consulted the 10/12/17 at:
https://ch.mathworks.com/help/pdf_doc/pde/index.html?s_cid=doc_ftr